FERMILAB-PUB-98/341-T
October 1998

Strong radiative corrections to $Wb\bar{b}$ production in $p\bar{p}$ collisions

R.K. Ellis and Siniša Veseli

Theory Group, Fermi National Accelerator Laboratory, P.O. Box 500, Batavia, IL 60510

Abstract

We calculate the strong radiative corrections to the process $p\bar{p} \to W(\to e\nu)g^*(\to b\bar{b})$. At the Tevatron this process is the largest background to the associated Higgs boson production $p\bar{p} \to W(\to e\nu)H(\to b\bar{b})$. The calculation is based on the subtraction procedure, and the corrections are found to be significant.

1 Introduction

The search for the origin of electroweak symmetry breaking is at the top of the agenda for the next generation of collider experiments. In the standard model (SM) the mechanism of electroweak symmetry breaking predicts the existence of a single uncharged Higgs boson whose mass is *a priori* unknown. It is currently constrained to be $90 < M_H < 280$ GeV at 95% confidence level [1], where the upper bound comes from precision electroweak measurements, while the lower bound is determined by direct searches.[1]

At the Tevatron collider there is the potential to look for the SM Higgs boson using the decay mode $H \to b\bar{b}$ [4]. In the lowest order (LO) the most promising process is

$$p\bar{p} \to W(\to e\nu)H(\to b\bar{b}) \ . \tag{1}$$

This search can cover the mass range up to about 130 GeV, once event samples, perhaps as large 30fb^{-1}, have been accumulated. Collection of data samples of this size will not be easy. However, the Tevatron search is of great importance, especially because the mass range between $100 < M_H < 130$ GeV is one of the most challenging regions for the LHC to look for the SM Higgs [5].

In this letter we calculate the strong radiative corrections to the $Wb\bar{b}$ process

$$p\bar{p} \to W(\to e\nu)g^*(\to b\bar{b}) \ , \tag{2}$$

which is the principal background for the associated Higgs production (1) at the Tevatron. Other non-negligible backgrounds, provided by the production of WZ, $t\bar{b}$, $t\bar{t}$ and other processes [4], will not be considered here. The calculation is performed in the limit where b-quark is massless, and our results indicate that the next-to-leading order (NLO) corrections to the $Wb\bar{b}$ background are significant.

[1] We note here that in the minimal supersymmetric extension of the standard model (MSSM) the Higgs boson mass is constrained to be less than about 130 GeV [2], and that for some range of parameters the neutral Higgs boson of the MSSM behaves like the Higgs boson of the standard model [3].

In Section 2 we briefly describe the calculation method based on the subtraction procedure [6], as formulated in [7]. Results for the NLO corrections to the lowest order processes (1) and (2) at the Tevatron are presented in Section 3, while conclusions are given in Section 4.

2 Calculation method

In order to evaluate the strong radiative corrections to processes (1) and (2) we have to consider Feynman diagrams describing real radiation, and also the ones involving virtual corrections to the tree level graphs.

The corrections due to real radiation are dealt with using the general subtraction algorithm formulated by Catani and Seymour [7], which is based on the fact that the singular parts of the QCD matrix elements for real emission can be singled out in a process-independent manner. By exploiting this observation one can construct a set of counter-terms that cancel all non-integrable singularities appearing in real matrix elements. The NLO phase space integration can then be performed numerically in four dimensions.

The counter-terms that were subtracted from the real matrix elements have to be added back and integrated analytically in n dimensions over the phase space of the extra emitted parton, leading to poles in $\epsilon = (n-4)/2$. After combining those poles with the ones coming from the virtual graphs all divergences cancel, so that one can safely perform the limit $\epsilon \to 0$ and carry out the remaining phase space integration numerically.

For the signal process (1) we consider only the effects of the initial state gluon emission.[2] The final state radiation can be taken into account in the total rate by using the radiatively corrected branching ratio for $H \to b\bar{b}$ [8]. The virtual corrections to (1) are of the Drell-Yan type and are well known [9, 10]. They are expressible as a multiple of the lowest order matrix element squared.

[2]Examples of Feynman diagrams which have to be taken into account for the signal and background processes are shown in Figures 1 and 2, respectively.

For the $Wb\bar{b}$ background process (2) we consider real radiation from both initial and final state quarks. The virtual corrections to the tree level graphs can be obtained by crossing the one loop helicity amplitudes for the process $e^+e^- \to \bar{q}q\bar{Q}Q$ [11].

Note that our final results are presented in the $\overline{MS}$ renormalization and factorization scheme. However, in intermediate steps for the $Wb\bar{b}$ process we used the four dimensional helicity scheme of [11].

For the sake of simplicity, we performed the calculation in the limit where b-quark is considered massless, and with CKM matrix elements V_{ub} and V_{cb} set to zero. In the case of $Wb\bar{b}$ background, the latter approximation eliminates the need to take into account scattering processes involving b-quarks in the initial state. Given that, for example, $|V_{cb}/V_{ud}|^2 \approx 0.002$, the effects of setting $V_{cb} = V_{ub} = 0$ are small. Corrections for the finite b-quark mass are expected to be of order $4m_b^2/M_{b\bar{b}}^2$, or about 1% for $M_{b\bar{b}} \sim 100$ GeV.

In order to ensure that we have a hard sub-process, we have also introduced a set of basic cuts,

$$\begin{aligned} (p_b + p_{\bar{b}})^2 &> 4Q^2 \,, \\ p_b^T &> Q \,, \\ p_{\bar{b}}^T &> Q, \end{aligned} \tag{3}$$

where Q is a scale of the same order as the b-quark mass. The first constraint imposes the correct physical threshold even though we have set the b quark mass to zero. The constraint on the p_T of the b and $\bar{b}$ quarks obviates the need for factorization subtractions involving the lowest order process $qb \to Wq'b$. In general, more stringent cuts on all three quantities will be required for comparison with experimental data.

3 Results

All results given in this paper report on the rate obtained for W^+ production in $p\bar{p}$ collisions at $\sqrt{S} = 2$ TeV. To include the contributions from W^- production and the contributions from the $W^\pm$ decay into muons, one should multiply our results by a factor of

four. Note however that we assume perfect efficiency ϵ_b for detection of b-jets. Achievable values of this efficiency would decrease our results by a factor of $\epsilon_b^2 \approx 0.2$ [12]. We used the MRSR2 parton distribution functions with $\alpha_S(M_Z) = 0.120$ [13], while the scale Q from (3) was set equal to 4.62 GeV.

In Figure 3 we first show the scale dependence of the LO and NLO cross sections for the signal and background processes in a mass window $84 < M_{b\bar{b}} < 117$ GeV, which is appropriate [4] for a 100 GeV Higgs boson. No other cuts apart from (3) have been applied. At a *natural* scale of $\mu = 100$ GeV we find that the K-factor is about 1.2 for the signal, but 1.5 for the background.

As already mentioned, more strict cuts than those of (3) have to be applied for comparison with experiment. In addition to the cuts on rapidity and transverse momentum,

$$\begin{aligned} |y_b|, |y_{\bar{b}}| &< 2 \ , \\ |y_e| &< 2.5 \ , \\ |p_b^T|, |p_{\bar{b}}^T| &> 15 \text{ GeV} \ , \\ |p_e^T|, |p_\nu^T| &> 20 \text{ GeV} \ , \end{aligned} \tag{4}$$

we also impose isolation cuts,

$$R_{b\bar{b}}, R_{eb}, R_{e\bar{b}} > 0.7 \ , \tag{5}$$

as well as a cut on the scattering angle of the $b\bar{b}$ system [14] (the Higgs scattering angle) in the Collins-Soper frame [15],

$$|\cos\theta_{b\bar{b}}| < 0.8 \ . \tag{6}$$

Note that imposing the cut on $\cos\theta_{b\bar{b}}$ requires knowledge of the longitudinal component of a neutrino momentum. By assuming that W boson is on shell, and using p_e and p_ν^T which are actually measured, this component can be reconstructed up to a two-fold ambiguity for a solution of a quadratic equation. Due to the asymmetry of the neutrino rapidity distribution, by choosing the larger (smaller) solution for p_ν^z in the case of W^+ (W^-), one can improve the probability of finding the correct W momentum. Following this

prescription, in our LO (NLO) Monte Carlo studies with the above cuts we have observed efficiency of about 77% (68%) and 70% (61%) for processes (1) and (2), respectively.[3]

Figures 4, 5 and 6 show our results obtained after cuts (4)-(6) have been imposed. In Figure 4 we illustrate the $b\bar{b}$ mass dependence of the $Wb\bar{b}$ process in LO and NLO. The shape of this curve, which is fairly insensitive to the particular choice of scale, could be important in extrapolating the $Wb\bar{b}$ background from observed events with lower $b\bar{b}$ invariant mass. Our scale choice of $\mu = 25\,\mathrm{GeV}$, for which the total LO and NLO cross sections are similar, allows one to approximately compare the shapes of the LO and NLO curves. Note that we have clustered the b-partons with emitted radiation to form b-jets.[4] Our results indicate that this procedure does not significantly alter the shape of the $b\bar{b}$ mass spectrum.

Figures 5 and 6 show the scale dependence of the LO and NLO cross sections for $84 < M_{b\bar{b}} < 117\,\mathrm{GeV}$ ($M_H = 100\,\mathrm{GeV}$) and $102 < M_{b\bar{b}} < 141\,\mathrm{GeV}$ ($M_H = 120\,\mathrm{GeV}$). At *natural* scales we estimate a signal to $Wb\bar{b}$ background ratio of 0.43 and 0.30 at $M_H = 100\,\mathrm{GeV}$ and $M_H = 120\,\mathrm{GeV}$, respectively. Before definitive conclusions can be drawn on the Tevatron search for the SM Higgs boson other backgrounds need to be included.

4 Conclusions

We have presented first results from a calculation of the radiative corrections to the production of $b\bar{b}$ in association with a W. The corrections are observed to be large and positive at *natural* scales. The full implications of this for the search for the standard model Higgs boson at the Tevatron will be discussed elsewhere [18]. Note that sizable

[3]The actual efficiency of accepting an event based on the calculated value of $\cos\theta_{b\bar{b}}$ from the reconstructed W momentum is higher. With cuts (4)-(6) we found that about 93% (87%) and 87% (79%) of the LO (NLO) events for processes (1) and (2) were correctly accepted or rejected.

[4]We have used the standard $k_\perp$-clustering algorithm [16, 17] with the cone size parameter $R = 0.7$.

corrections have also been found in other reactions where the same virtual matrix elements have been used in a crossed channel [19, 20]. As yet we have no clear analytic understanding of why this should be so.

Our calculation can be considered the first step in the calculation of $W + 2$ jet cross section. In addition, extension of our programs to other two boson processes should be straightforward.

Acknowledgements

We are happy to acknowledge useful discussions with L. Dixon, M. Mangano, S. Parke and M. Seymour. Fermilab is operated by URA under DOE contract DE-AC02-76CH03000.

References

[1] D. Carlen, ICHEP98, Vancouver, July 1998;
D. Treille, ICHEP98, Vancouver, July 1998.

[2] M. Carena *et al.*, *Phys. Lett.* **B355**, 209 (1995), *Nucl. Phys.* **B461**, 407 (1996);
H. Haber *et al.*, *Zeit. Phys.* **C57**, 539 (1997).

[3] M. Carena *et al.*, hep-ph/9808312.

[4] A. Stange, W. Marciano and S. Willenbrock, *Phys. Rev.* **D49**, 1354 (1994), *Phys. Rev.* **D50**, 4491 (1994);
S. Kuhlmann, TeV2000 report.

[5] ATLAS Technical Proposal, CERN/LHCC 94-43, 1994;
CMS Technical Proposal, CERN/LHCC 94-38, 1994.

[6] R.K. Ellis, D.A. Ross and A.E. Terrano, *Nucl. Phys.* **B178**, 421 (1981).

[7] S. Catani and M.H. Seymour, *Nucl. Phys.* **B485**, 291 (1997), Erratum *Nucl. Phys.* **B510**, 503 (1997).

[8] A. Djouadi, J. Kalinowski and M. Spira, *Comp. Phys. Comm.* **108**, 56 (1998).

[9] G. Altarelli, R.K. Ellis and G. Martinelli, *Nucl. Phys.* **B157**, 461 (1979).

[10] T. Han and S. Willenbrock, *Phys. Lett.* **B273**, 167 (1991).

[11] Z. Bern, L. Dixon, D. Kosower and S. Weinzierl, *Nucl. Phys.* **B489**, 3 (1997);
Z. Bern, L. Dixon and D. Kosower, *Nucl. Phys.* **B513**, 3 (1998).

[12] *The CDFII detector*, Technical Design Report, Fermilab-Pub-96/360-E.

[13] A.D. Martin, R.G. Roberts and W.J. Stirling, *Phys. Lett.* **B387**, 419 (1996).

[14] S. Kim, S. Kuhlmann and W.M. Yao, presented at 1996 DPF/DPB Summer Study on New Directions for High-energy Physics (Snowmass 96), Snowmass, CO, July 1996;
P. Agrawal, D. Bowser-Chao and K. Cheung, *Phys. Rev.* **D51**, 6114 (1995).

[15] J.C. Collins and D. Soper, *Phys. Rev.* **D16**, 2219 (1977).

[16] S. Catani, Yu.L. Dokshitzer, M.H. Seymour and B.R. Webber, *Nucl. Phys.* **B406**, 187 (1993).

[17] S.D. Ellis and D.E. Soper, *Phys. Rev.* **D48**, 2160 (1993).

[18] R.K. Ellis and S. Veseli, in preparation.

[19] L. Dixon and A. Signer, *Phys. Rev.* **D56**, 4031 (1997).

[20] Z. Nagy and Z. Trocsanyi, hep-ph/9806317.

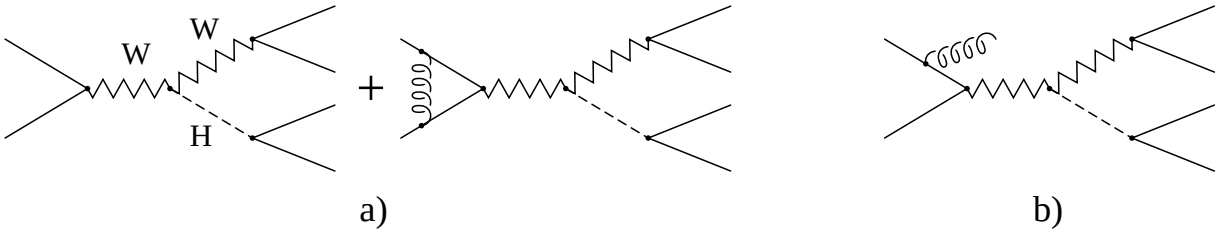

Figure 1: Examples of Feynman diagrams which have to be taken into account for the WH signal. Diagrams a) correspond to the tree level process plus the virtual contribution, while diagram b) corresponds to the real emission process.

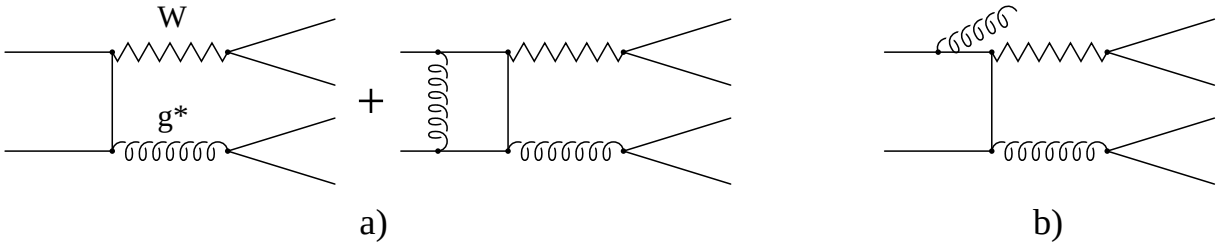

Figure 2: Examples of Feynman diagrams which have to be taken into account for the $Wb\bar{b}$ background. Diagrams a) correspond to the tree level process plus the virtual contribution, while diagram b) corresponds to the real emission process.

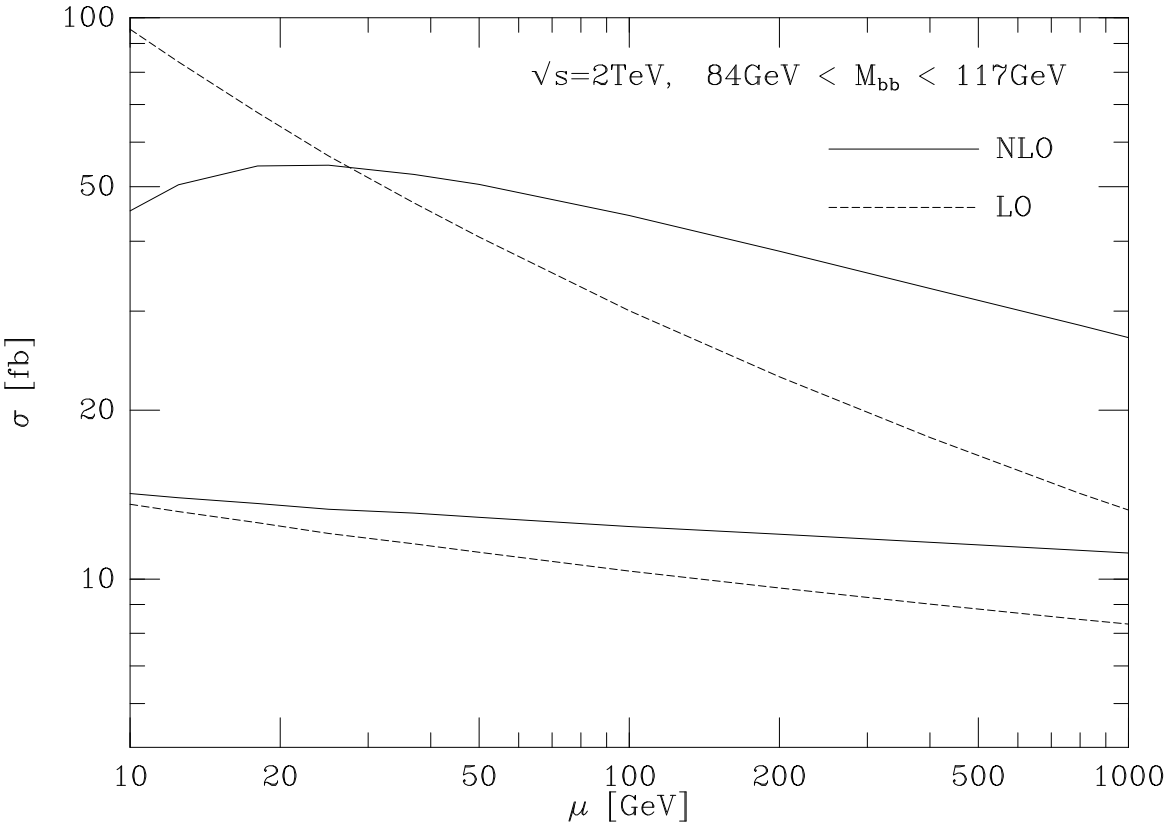

Figure 3: Cross section scale dependence for the signal (lower curves) and $Wb\bar{b}$ background (upper curves). These results were obtained for $84 < M_{b\bar{b}} < 117$ GeV ($M_H = 100$ GeV). Apart from (3), no other cuts have been applied.

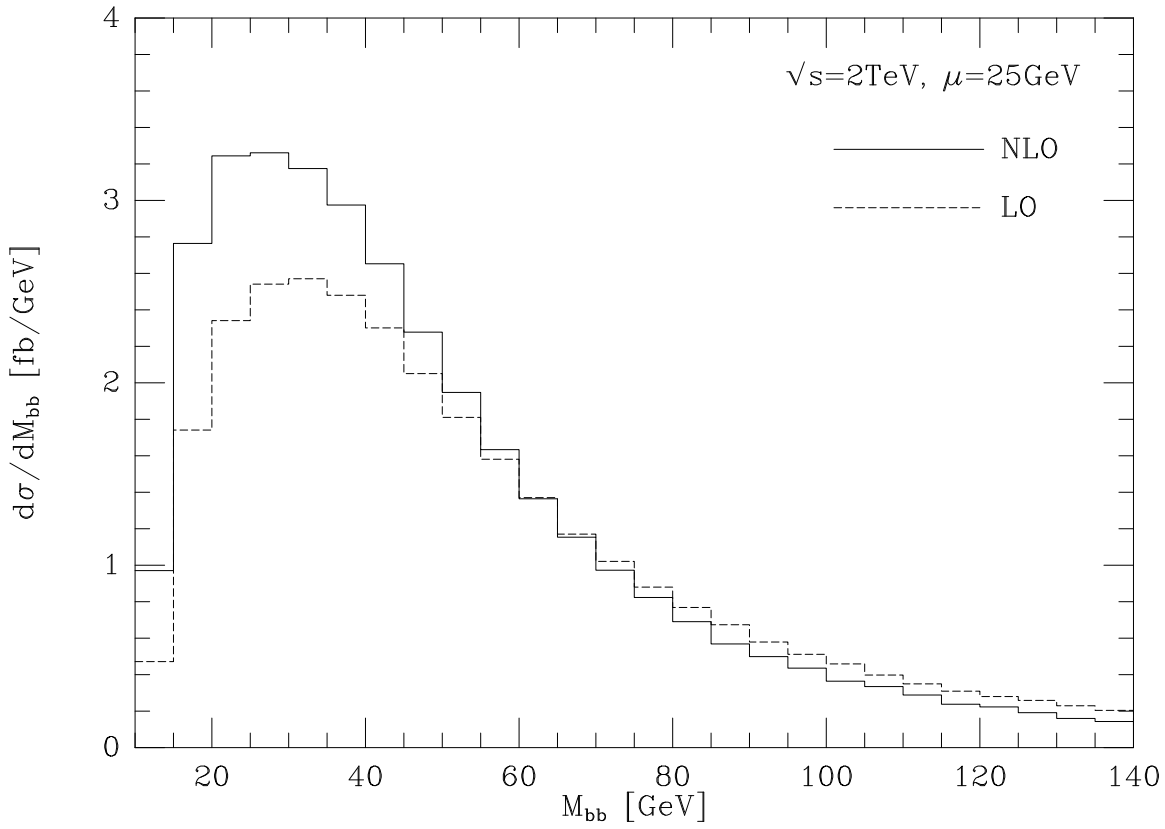

Figure 4: The LO and NLO $M_{b\bar{b}}$ dependence of the $Wb\bar{b}$ background process at a scale of $\mu = 25$ GeV. The results shown were obtained after imposing cuts given in (4)-(6).

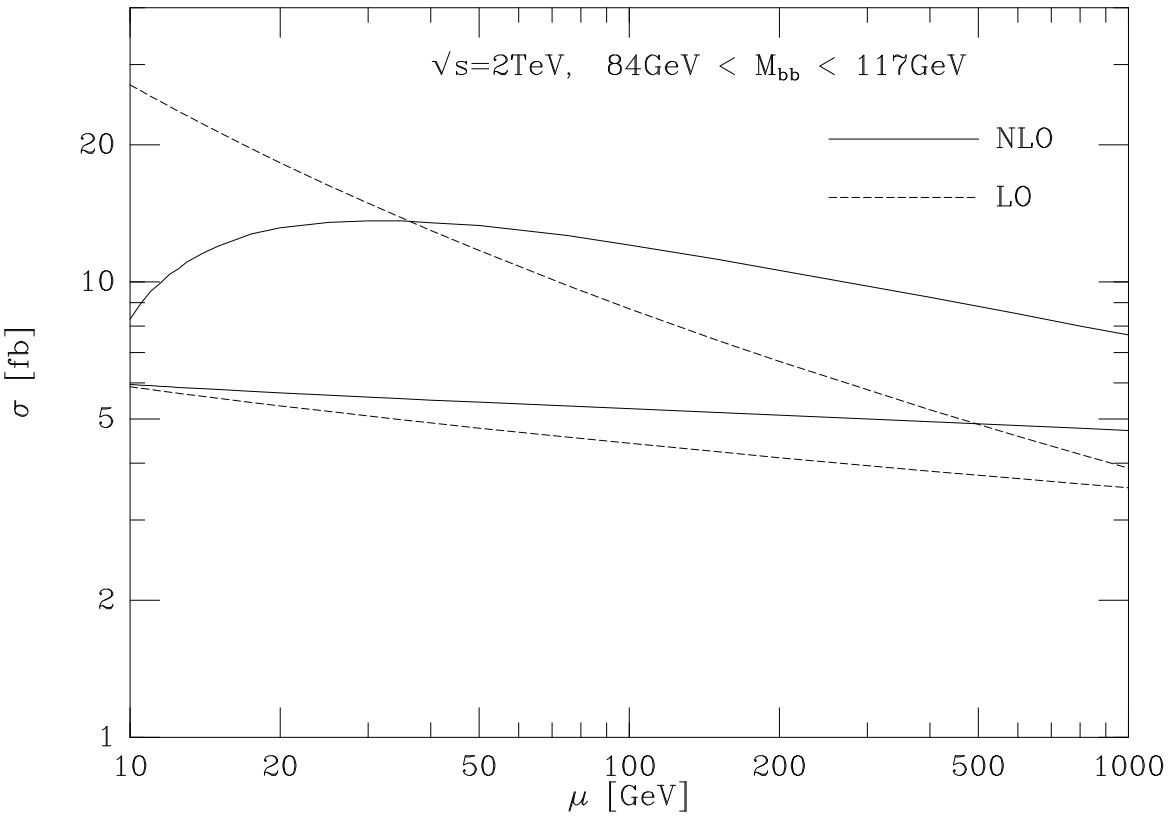

Figure 5: Cross section scale dependence for the signal (lower curves) and $Wb\bar{b}$ background (upper curves). These results were obtained for $84 < M_{b\bar{b}} < 117$ GeV ($M_H = 100$ GeV), and after imposing cuts given in (4)-(6).

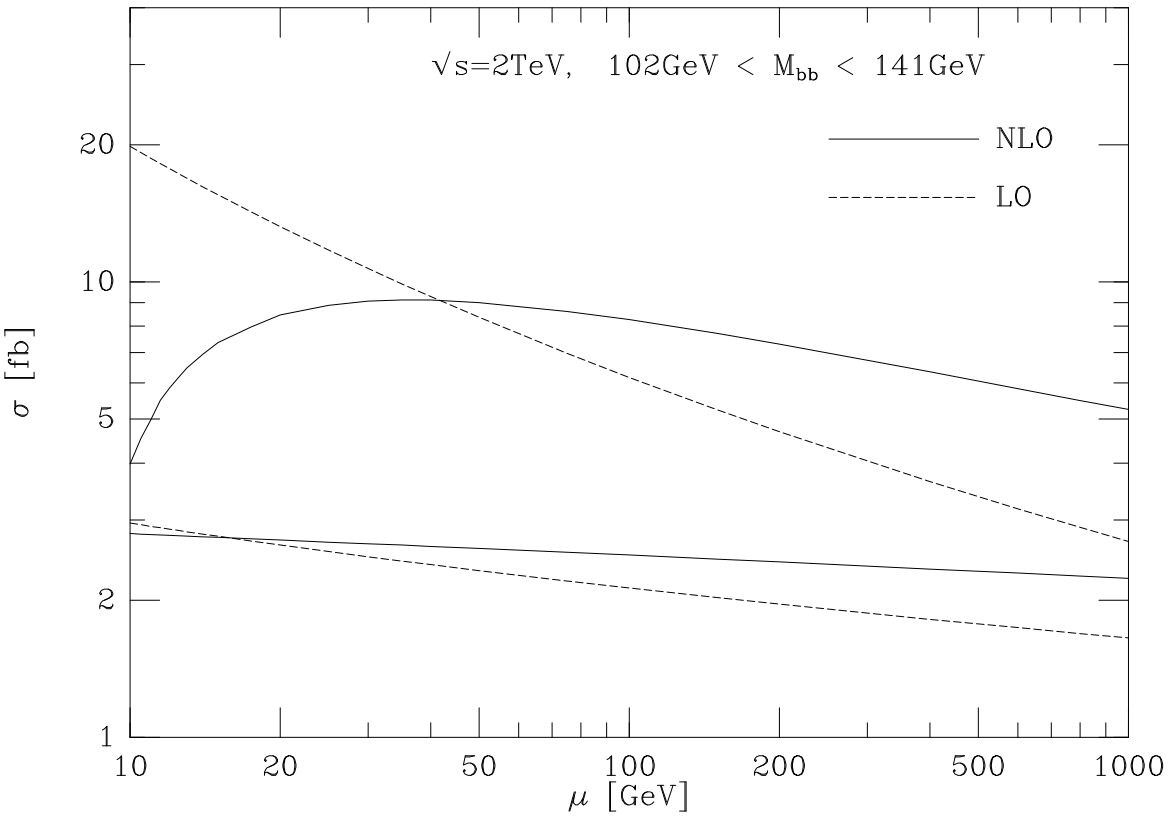

Figure 6: Cross section scale dependence for the signal (lower curves) and $Wb\bar{b}$ background (upper curves). These results were obtained for $102 < M_{b\bar{b}} < 141$ GeV ($M_H = 120$ GeV), and after imposing cuts given in (4)-(6).